JOURNAL OF OPTOELECTRONICS AND ADVANCED MATERIALS Vol. 12, No. 9, September 2010, p. 1899 - 1902

Influence of heat treatment atmosphere on the superparamagnetic iron oxide – hydroxyapatite composites

C. MIRESTEAN, P. BERCE[a], S. SIMON[*]
Babes-Bolyai University, Faculty of Physics & Institute for Interdisciplinary Research in Bio-Nano-Sciences, 400084 Cluj-Napoca, Romania
[a]*Technical University, Faculty of Machine Building & National Centre of Rapid Prototyping, 400641 Cluj-Napoca, Romania*

Hydroxyapatite with 20 mol % Fe_2O_3 was synthesized following the coprecipitation route. Heat treatment at 700 ^oC in either air or nitrogen flux was applied in order to develop finely dispersed superparamagnetic particles, either hematite or magnetite in the biocompatible hydroxyapatite phase. The X-ray diffraction patterns demonstrated the development of hydroxyapatite with crystallites size about 40 nm . The developed superparamagnetic particles have been proved by EPR as being mainly hematite in the case of normal air atmosphere, and magnetite in the case of nitrogen atmosphere.

(Received August 25, 2010, after revision September 3, 2010; accepted September 15, 2010)

Keywords: Hydroxyapatite, Superparamagnetic iron oxides, XRD, EPR

1. Introduction

A key requirement in the field of bone tissue engineering is the development of scaffold structures on which cells adhere. As prevalent component of the bones, the hydroxyapatite (HA) is introduced in almost all scaffolds designed for bone repairing [1-4]. Iron doped hydroxyapatite (HA-Fe) is considered for the hyperthermia treatment of bone tumors in form of permanent implants [5-8]. In the last few years new fabrication methods, called rapid prototyping techniques, have been developed for the fabrication of hydroxyapatite scaffolds for bone substitutes or tissue engineering applications. With this generative fabrication technology an individual tailoring of the scaffold characteristics can be realised [9-11].

The hydroxyapatite embedded in a living bone has a high affinity to surrounding tissue, and the ferrimagnetic particles exhibits a highly efficient magnetically inducted heat generation in an alternative magnetic field, without realising noxious ions therefrom [12]. The heat-generating iron doped hydroxyapatite is particularly useful for deep cancers like bone tumors, and can be applied in various shapes as powder, shaped bulk form or fiber depending on administration means, and can be used continuously or for a long period without an adverse influence. The development of magnetic phases is aimed in the host matrix. The presence of both Fe^{3+} and Fe^{2+} ions can be influenced by the oxidative character of the heat treatment atmosphere, and can favour the nucleation of the magnetite phase [6]. Significant attention continues to be given to research of superparamagnetic particles of magnetite and hematite with applications for hyperthermia [13-16].

This study aims to investigate the effect of 700^0C heat treatment carried out in either air or nitrogen atmopshere on the iron valence states and superparamagnetic phase development in iron containing hydroxyapatite.

2. Experimental

Hydroxyapatite (HA) samples with 20 mol % Fe_2O_3 were prepared from $(NH_4)_2HPO_4$, $Ca(NO_3)_2 \cdot 4\ H_2O$, and $Fe(NO_3)_3 \cdot 9H_2O$, using the precipitation route. In a 0.2 M $(NH_4)_2HPO_4$ solution was added droplet by droplet a 0.2 M $Ca(NO_3)_2 \cdot 4H_2O$ solution, and under continuos stirring at 90 ^oC were introduced the droplets of 0.2 M $Fe(NO_3)_3 \cdot 9\ H_2O$ solution. The heating continued up to the evaporation of the water. The resulting precipitate was dried at 120 ^oC for 24 hours, and then the samples were treated at 700 ^oC in a tubular Carbolite furnace both in normal air atmosphere and in nitrogen atmosphere.

The dried samples were analysed on a Shimadzu DTG-6OH derivatograph at the heating rate of 10ºC/min, up to 900 ^oC. The structure analysis of the samples was performed on a Shimadzu XRD 6000 X-ray diffractometer, with a Ni–filter, using CuK_α radiation (λ = 1.5418Å). The operation voltage and current were 40 kV and 30 mA. The measurements were performed at a scan speed of 1^o/min. The crystallites size has been estimated by using Scherrer formula [17]. Electron paramagnetic resonance measurements were performed at room temperature on an ADANI spectrometer operating at 9.4 GHz (X-band).

3. Results and discussion

The thermal analysis evidenced several events up to 700 °C (Fig. 1) mainly related to removal of physical adsorbed water, up to 135 °C, with a mass loss of 18.3 %, residual nitrates decomposition and dehydroxylation, around 534 °C, with a mass loss of 15.6 %. The weak exothermic peak at 675 °C denotes a structural rearrangment in sample, and for this reason the 120 °C dried samples were treated at 700 °C, in normal air atmosphere as well as in nitrogen atmosphere. The colour of the samples changed from a light yellow to reddish after the 700 °C treatment in air, whereas the colour changed to greyish when the sample was heated at the same temperature in nitrogen atmosphere.

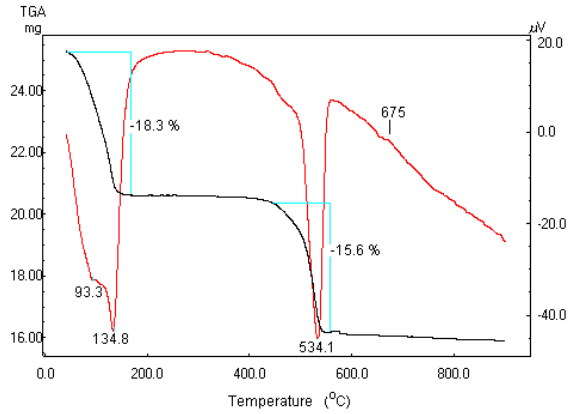

Fig. 1. DTA and TG curves of coprecipitated hydroxyapatite containing 20 mol% Fe_2O_3.

The X-ray diffraction patterns of the composite HA-Fe (Fig. 2) show differences for the samples heated in different atmospheres. The diffractogram of the sample heated in air shows well developed crystals of hydroxyapaptite type, with size about 40 nm, while the diffraction lines recorded from the sample heat-treated in nitrogen are broader and denote smaller crystallites, with size about 15 nm. At the same time, for the sample heated in nitrogen is observed a change in relative peak intensities at 31.7° and 32.9° as well as a new peak at 34.7°, that can be due to the contribution from hematite and magnetite phase, respectively. On the other hand, the absence of clear evidence for hematite or magnetite phases [18] may by considered under two assumptions: *(i)* either iron ions are incorporated into the hydroxyapatite lattice at calcium sites, or *(ii)* hematite or magnetite phases are not detected by X-ray diffraction due to the very small crystallite size. Earlier studies [19] reported on iron oxides present in oxide compounds without to be evidenced by X-ray diffraction analysis due to the fact that they occured as very fine particles labelled „free" iron oxides, and that is the case of superparamagnetic particles that can be evidenced by electron paramagnetic resonance (EPR).

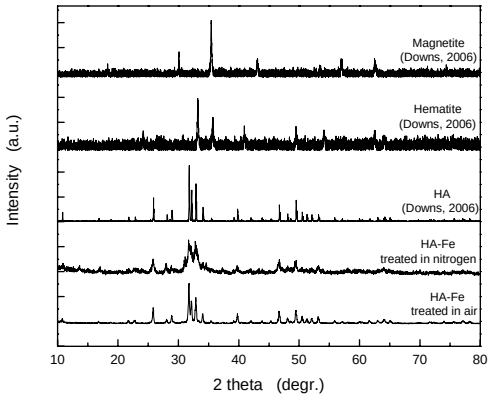

Fig. 2. X-ray diffraction patterns of the samples treated at 700 oC in air and nitrogen atmosphere, snd the reference patterns for hydroxyapatite (HA), hematite and magnetite.

The EPR analysis carried out at room temperature inform mainly on Fe^{3+} ions ($3d^5$, $^6S_{5/2}$), and indirectly on the Fe^{2+} ions with which the ferric ions interact and therefore the EPR linewidth will have to be evaluated. The EPR spectrum of the samples heated at 550 °C (Fig. 3) shows two resonance lines at g = 4.3 and 2.0. The first line, at g = 4.3, is assigned to isolated Fe^{3+} ions in sites of low symmetry characterized by high crystal fields, distributed in HA's structure, and that at g = 2.0 to Fe^{3+} ions in sites of octahedral symmetry, with low crystal fields and to iron ions that are experiencing strong dipolar and/or superexchange interactions [20-23]. The intensity of g = 2.0 line is diminished as the sample was treated in nitrogen, denoting less ferric ions than in the sample treated in air. Moreover, the line broadening can be assigned to the interaction of ferric and ferrous ions, in the assumption that part of Fe^{3+} ions were converted into Fe^{2+} ions during the treatment in nitrogen atmosphere.

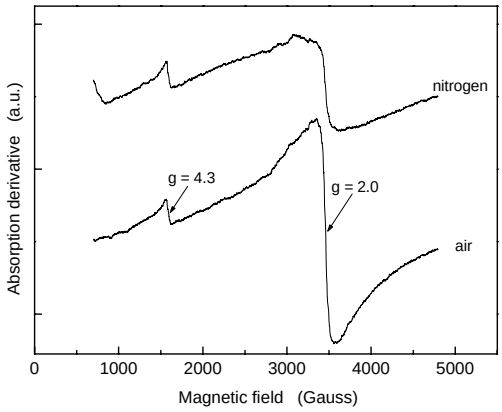

Fig. 3. EPR spectra of the samples treated at 550 °C in air and nitrogen atmosphere.

Regardless of the 700 ^{o}C treatment atmosphere, the g = 4.3 resonance line does not more observed in the EPR spectra (Fig. 4) which are dominated by the very strong line with g = 2.0. There are evident differences in the shape of g = 2.0 lines recorded from these samples. For the samples heated in air the line is narrow, about 100 G, and symmetric, while the g = 2.0 resonance line recorded from the sample heated in nitrogen appears as a superposition of two contributions, one related to a narrow signal, like in the case of the sample heat treated in air, and another one related to a large and asymmetric signal, with the linewidth around 900 G. The resonance lines at g = 2 which are narrower than the 200 G are considered typical of a superparamagnetic phase like hematite [16, 24, 25], while the larger and asymmetrical line is associated with magnetite particles [20].

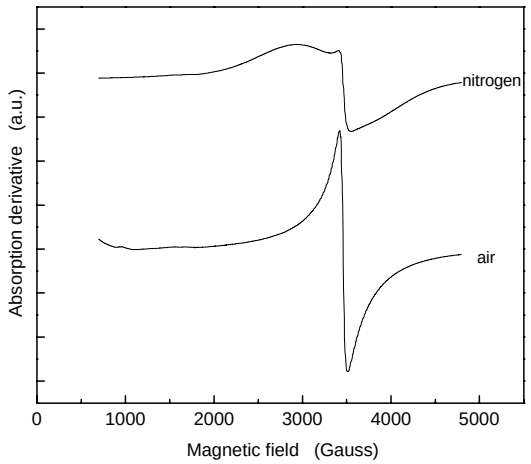

Fig. 4. EPR spectra of the samples treated at 700 ^{o}C in air and nitrogen atmosphere.

The different colours of the samples treated in air and nitrogen, are in good agreement with the EPR results. Superparamagnetic iron particles mainly affect the colour of aluminosilicate systems, like clays [18, 25]. The presence of superparamagnetic hematite in the air treated sample confers a reddish colour to the sample, while the presence of superparamagnetic magnetite as a major magnetic phase in the sample heat treated in nitrogen atmosphere gives a grey colour to the sample.

4. Conclusion

Nano iron oxide - hydroxyapatite composites were synthesized by coprecipitation method and heat treatment at 700 ^{o}C in air or nitrogen atmosphere. XRD results showed that the size of the hydroxyapatite crystallites were smaller when the treatment was performed in nitrogen, as compared with the sample treated in air. The analysis of EPR spectra pointed out on the coexistence of paramagnetic Fe^{3+} ions and superparamagnetic particles, and supported that only a small part of iron ions entered in calcium sites of hydroxyapatite, while the majority occurred as iron oxides in very small sized particles. Heat treatment applied in air atmosphere at 700 ^{o}C enabled to produce a finely dispersed superparamagnetic hematite particles in the biocompatible hydroxyapatite phase, while after treatment at the same temperature in nitrogen superparamagnetic magnetite particles are preponderantly developed.

Acknowledgements

This work was supported by CNCSIS Romania, under PN II IDEI - PCCE 101/2008 project.

References

[1] M. Ajeesh, B. F. Francis, J. Annie, P. R. Harikrishna Varma, J. Mat. Sci. Mater. Med., **21**(5), 1427 (2010)
[2] G. Socol, A. M. Macovei, F. Miroiu, N. Stefan, L. Duta, G. Dorcioman, I.N. Mihailescu, S. M. Petrescu, G. E. Stan, D.A. Marcov, A. Chiriac, I. Poeata, Mat. Sci. Eng. B, **169**(1-3), 159 (2010)
[3] K. Niespodziana, K. Jurczyk, J. Jakubowicz, M. Jurczyk, Mat. Chem. Phys., **123**(1), 160 (2010).
[4] G. E. Stan, J .M. F. Ferreira, J. Optoelectr. Adv. Mater., **9**(8), 2539 (2007).
[5] K. A. Gross, R. Jackson, J. D. Cashion, L. M. Rodriguez-Lorenzo, Eur. Cells Mater., **3**(S2), 114 (2002).
[6] D. Eniu, D. Cacaina, M. Coldea, M. Valeanu, S. Simon, J. Magn. Magn. Mater. **293**(1), 310 (2005).
[7] C. Mirestean, H. Mocuta, R. V. F. Turcu, G. Borodi, S. Simon, J. Optoelectr. Adv. Mater., **9**(3), 764 (2007).
[8] D. Predoi, M. Barsan, E. Andronescu, R. A. Vatasescu-Balcan, M. Costache, J. Optoelectr. Adv. Mater. **9**(11), 3609 (2007).
[9] U. Deisinger, F. Stenzel, J. Lehmann, G. Ziegler, Technol. Health Care, **12**(2), 108 (2004).
[10] G. Daculsi, P. Layrolle, Key Eng. Mater. **361-363**, 915 (2007)
[11] A. Ott, F. Irlinger, Int. J. Comput. Technol. **36**(1), 32 (2009)
[12] W. Pon-On, S. Meejoo, I. M. Tang, Int. J. Nanosci. **6**(1), 9 (2007).
[13] P. Cantillon-Murphy, L. L. Wald, M. Zahn, E. Adalsteinsson, Concept Magn. Reson. A**36**(1), 36 (2010)
[14] P. Cantillon-Murphy, L. L. Wald, E. Adalsteinsson, M. Zahn, J. Magn. Magn. Mater. **322**(6), 727 (2010).
[15] P. Cantillon-Murphy, L. L. Wald, E. Adalsteinsson, M. Zahn, J. Magn. Magn. Mater. **322**(17), 2607 (2010).

[16] I. R. Macdonald, R. F. Howe, S. Saremi-Yarahmadi, K. G. U. Wijayantha, J. Phys. Chem. Lett., **1**, 2488 (2010).
[17] A. L. Patterson, Phys. Rev. **56**(10), 978 (1939).
[18] J. Komusinski, L. Stoch, S.M. Dubiel, Clay Clay Miner., **29**(1), 23 (1981).
[19] R. T. Downs, The RRUFF Project: an integrated study of the chemistry, crystallography, Raman and infrared spectroscopy of minerals, Program and Abstract of the 19th General Meeting of the International Mineralogical Association in Kobe, Japan. O03-13, 2006.
[20] D. L. Griscom, J. Non-Cryst Solids, **67**, 81 (1984).
[21] J. Kliava, R. Berger, Y. Servant, J. Emery, J. M. Greneche, J. Non-Cryst. Solids **202** (3), 205 (1996).
[22] R. Berger, J. C. Bissey, J. Kliava, H. Daubric, C. Estournes, J. Magn. Magn. Mater. **234**(3), 535 (2001).
[23] S. Simon, R. Pop, V. Simon, M. Coldea, J. Non-Cryst. Solids, **331** (1-3) 1 (2003).
[24] I. Edelman, J. Kliava, Physica Status Solidi (b), **246**(10), 2216 (2009).
[25] L. C. Bertolino, A. M. Rossi, R.B. Scorzelli, M. L. Torem, Appl. Clay Sci., **49**(3), 170 (2010).

*Corresponding author: simion.simon@phys.ubbcluj.ro